

Interactive comment on “Magma mixing enhanced by bubble segregation” by S. Wiesmaier et al.

S. Wiesmaier et al.

sebastian.wiesmaier@min.uni-muenchen.de

Received and published: 26 June 2015

Dear Prof. Arndt, reviewers and readers following this discussion, We would like to thank the two reviewers for their constructive comments and the thought-stimulating nature of these. In the following, we will answer to each of these comments separately. In the attached pdf, our rebuttal is written in bold type and consists of a) the answer to the reviewer's comments and b) in blue, when applicable, the proposed changes for the manuscript. The main body of text has now been condensed considerably and shortened to 8552 words (from 9330 words previously). Also, Figures 1, 2, 3 and 9 were changed to reflect the requests by the reviewers and are greatly improved now. With best regards, Sebastian Wiesmaier

Interactive comment on “Magma mixing enhanced by bubble segregation” by S. Wiesmaier et al. Anonymous Referee #1 Received and published: 11 May 2015 Referee #1:

C820

This manuscript presents new experimental data relevant to magma mixing processes operating in magmatic systems. Specifically, the authors have set out to explore efficacy of magma mixing when it is driven by bubble transport and these experiments are a complement to previous studies which have been numerical in nature or based on analogous fluids. The high-temperature experiments involve a lower cylinder of basalt overlain by a cylinder of basalt. The properties of the two melts are fully characterized prior to the experiments. The experiments are isothermal and the temperatures have been chosen carefully on the basis of the rheology of the two melt and in order to ensure no crystallization. The bubbles are a partly serendipitous in that they derive from the air trapped at the melt interface. The experiments involve holding the two layered melts (plus air bubbles) at fixed temperature for prescribed amounts of time. During this time, bubbles form, coalesce and rise; bubbles originating within the basalt or at the basalt-rhyolite interface rise and pull up tendrils or filaments of lower viscosity basaltic melt. The filaments rising into the rhyolite comprise a magma mixing mechanism involving advective transport of basalt (mingling) and chemical diffusion (mixing). Run products are sectioned perpendicular to the vertical axis to allow chemical and physical study of the filaments in cross-section. The manuscript provides full qualitative and quantitative description (physical and chemical) of the filaments. Their analysis includes petrographic analysis, micro-computed tomographic imaging and electron microprobe analysis. These data are then used to compare the experimental results to the literature - especially the numerical modelling of bubble ascent (e.g. Manga & Stone). They also use these observations to establish the complex dynamic processes involved in the bubble rise and basalt melt infiltration of filaments into the rhyolite. The manuscript concludes with a full discussion of the applicability of these processes to nature - to what extent can bubble migration contribute to magma mixing in natural systems. Overall the manuscript is well organized, well-written and illustrated. The arguments are by and large convincing. There are however a number of areas where I suggest the manuscript and arguments could be clarified. My suggestions are listed below.

C821

[Authors' comments:] We are pleased to hear that the reviewer deems our work a full qualitative and quantitative description of the filaments, complemented by convincing arguments.

Referee #1: 0) the manuscript could be improved overall with another editing.

[Authors' comments:] The manuscript has been proof-read and edited once more to condense and clarify language and text.

Referee #1: 1) Introduction: The introduction should be rewritten. Currently, the introduction is not really an introduction to the paper. It is actually more a review of magma mixing ideas. I recommend a short introduction to this paper - the question, the data, the goal. This can then be followed by a new section that summarizes all these ideas.

[Authors' comments:] We thank the reviewer for the suggestion to shorten the introduction. For the current text, we felt it important to introduce the reader properly to the distinction of physical mingling from chemical equilibration/diffusion, the two essential components of chaotic mixing. We therefore welcome the idea of the reviewer to shorten the introduction and place the discussion of magma mixing concepts into a new section that follows the discussion. Changes proposed for manuscript: "Page 1471-line 10 through 1473-25 will form a new section called "Background on chaotic mixing" The remaining text in the introduction has been adjusted for suitability as introduction.

Referee #1: 2) Vocabulary: I found that I had to read some of the text several times to find out what you actually meant with some terms. I think you need to revise text to define terms better and perhaps add a sketch figure to existing figures to make sure the reader is able to keep up. Bubbles rise / they entrain melt to create vertical filaments / the run products are sectioned horizontally to intersect filaments / EMP analyses transect the filament cross-sections.

C822

[Authors' comments:] Same as comment 0): The manuscript has now been proof-read and edited once more to condense and clarify language and text.

Referee #1: 3) Experimental set-up and other places I think it is worth defining the dimensionless numbers Re , Bo , Mo so that the reader is reminded which physical properties are involved.

[Authors' comments:] Accepted. In order to save space, and because we did not explicitly mention any calculated values of Mo (but instead refer to Clift et al. 2005), we gave equations of Re and Bo number only. The Mo number is still explained, just without equation. The following text has been included in section 3.2: Fluid dynamic parameters We employed several dimensionless numbers and the framework of Manga & Stone (1995) to constrain the experiment fluid dynamically. The dimensionless Reynolds number Re is the ratio of inertial to viscous forces and describes the flow regime of a fluid dynamical problem. For a sphere in a fluid, the characteristic length scale L is the radius of the sphere (here: bubble), the velocity v is Stokes' terminal settling velocity, and ρ and μ are density and viscosity of the fluid (Eq. 1).

The dimensionless Bond number Bo , also called Eötvös number, is used in combination with the Morton number Mo to describe the shape of a bubble or drop in a fluid. The Bo number is defined as ratio of the bodily forces to the surface tension affecting the bubble, with $\Delta\rho$ the density difference between fluid and bubble, g the gravitational acceleration, L the radius of the bubble and σ the surface tension of the fluid (Eq. 2).

Referee #1: 4) Section 2.4 The first few sentences are complex and unclear. I think you are saying: "After each experiment, the glass cylinders are sectioned at 3 locations parallel to the basalt-rhyolite interface".

[Authors' comments:] Yes, that is what we meant, accepted and change made. Combined with reviewer #1's comment 7), the previous text has been replaced with the following: Discs of experimental glass were prepared as electron microprobe mounts. One or several filaments per microprobe mount were analysed for major element con-

C823

centrations using a Cameca SX100 electron microprobe at LMU Munich.

Referee #1: 5) Section 2.7 The thickness is defined by the inflection points in the SiO₂ vs. distance curves.

[Authors' comments:] Accepted and change made. New sentence: Therefore, the thickness of filaments has arbitrarily been defined as the distance between the inflection points in the SiO₂ versus distance curves.

Referee #1: 6) Section 3.1 Line 23: for visibility $\hat{A}\hat{Z}\hat{A}$ or $\hat{A}\hat{Z}\hat{A}$ for illustrative purposes

[Authors' comments:] "visibility" replaced with "for illustrative purposes"

Referee #1: 7) Section 3.2 line 10-12. This is repeat - so you could simply state this only once (say it here and not in section 2.4)

[Authors' comments:] Accepted, text deleted from section 2.4.

Referee #1: 8) Section 3.2.2 I think you can do a much better job to connect these transects to Figure 4 - see my comments on the figure. It took me a long time to even see the transects in figure 4. I didn't know to look.

[Authors' comments:] The transects in Figure 4 have now been made much clearer and a key to the figure has been added, too. Also, references to Figures 4 a – c have been added to the section the reviewer mentioned.

Referee #1: 9) section 4.2 Lineline 25 "Stokes law correlates linearly with viscosity" I think this should be " Stokes Law velocities are proportional to 1/viscosity"

[Authors' comments:] Accepted, text changed to: "...as Stokes' Law velocities are proportional to 1/viscosity."

Referee #1: 10) Section 4.3.1 Here is another idea on interpreting the compositional profiles. As the plumes rise they are creating a longer and longer interface against the enclosing rhyolite melt. The extent of diffusion during the rise will increase as the

C824

tendrils gets longer. This is the same as during heat flow that the longer magma transits a dyke system the more heat is conducted into the wall rocks. You might consider this effect in terms of interpreting the compositional profiles.

[Authors' comments:] The reviewer is right, and this is exactly the pitfall between single- and multi-pulse filaments that we are trying to resolve. What reviewer #1 describes here is the formation of a single-pulse filament. One single pulse of magma, advected by a bubble, with the filament continuously stretching out while the bubble moves to the top. Bottom levels of vertical, cylindrical filaments then ought to be more equilibrated than upper levels, simply because of their longer time of equilibration. The diameter of the filament would be expected to be roughly constant, at best we estimate it to vary within an order of magnitude, from bottom to top. We agree 100% that this is most likely the correctly described mechanism for a single pulse filament. However, we don't find evidence for this in our experimental charge. 3D and compositional observations in turn point towards many multi-pulse filaments. Single pulse filaments should be more equilibrated at bottom levels in the experimental charge. In contrast, in Fig. 8, we observe filaments from the intermediate level (halfway between basalt-rhyolite interface and top of the rhyolite) to be bracketed in their degree of homogenization by filaments from the bottom-most level. We refrained so far from discussing the single pulse case in too much detail, as our argumentation begins by mentioning first-hand 3D visual evidence for multi-pulse filaments (see sections 4.1 of the revised manuscript (section 3.1 previously) and section 5.1 and 5.2 (previously 4.1 and 4.2)). To accommodate the reviewer's request, we included the following paragraph in section 5.3.1 (previously 4.3.1): We present a method to detect multi-pulse filaments in natural samples. For our experimental run products, the 3D visual evidence demonstrates that multi-pulse filaments are present. Nevertheless, in natural samples, 3D visual evidence may not be as clear cut as here. We thus aim to constrain the origin of filaments further by a statistical treatment of the compositional profiles obtained from EMP analysis. In the context of our experimental set-up, single-pulse filaments are expected to stretch out from the basalt-rhyolite interface towards the top of the rhyolite, as one bubble moves upwards

C825

within the rhyolite. Diffusional equilibration for single-pulse filaments thus ought to shift systematically from high degrees of equilibration at the bottom of a vertical, cylindrical filament to less degrees of hybridisation at the top. Such systematic correlation of diffusion-based equilibration with vertical position would be useful for constraining the time-scales of filament formation, but is not detected on our experimental filaments. Instead, rheologic and visual constraints show that experimental filaments formed by bubble mixing experienced multiple bubbles rising through. Such repeated replenishment of multi-pulse filaments with fresh end-member melt must affect the diffusional equilibration from previous pulses, though. Multi-pulse filaments are thus expected to significantly deviate in their diffusional behaviour from single pulse filaments. This is important because the calculation of magmatic time-scales based on diffusion gradients has commonly been based on a single pulse origin of magmatic filaments, bar other options recognized so far. It is thus vital to be able to distinguish single- from multi-pulse filaments in natural samples.

Referee #1: 11) Section 4.3.2 Line 10-15. When you are describing Figure 8 you should refer to the previous figure which shows the concave down model curves. Also I notice the scales are very different - any explanation for this discrepancy. Would your observed curves ultimately become concave down?

[Authors' comments:] Agreed, and reference to Fig. 6 added. As diffusional equilibration behaves systematically, the upward convex shape of the model filaments' equilibration (single-pulse) is not reversible. Very thin filaments must equilibrate very rapidly (given all other parameters are the same). The scales on the y-axes of Fig.6 and 8 are different, because concentration variance among different elements scales with their values of diffusivity. For example, Mg must reach much lower values for σ^2 than Si in the same filament due to its slightly higher diffusivity. Also, diffusivity values are highly dependent on the matrix composition. The multi-pulse origin of the filaments must obscure the correlation of diffusivity values with concentration variance for the same filament. We now included the following improved text in section 5.3.2 (pre-

C826

ously 4.3.2): Figure 8 shows concentration variance versus filament thickness for the four bell-shaped compositional profiles from the bubble mixing experiment. The regression curves of their concentration variance σ^2 has the opposite curvature (downwards convex) compared to the single-pulse modelled data (upward convex; see Fig. 6). This systematic dissimilarity indicates equilibration behaviour for the experimental filaments was fundamentally different compared to single-pulse filaments. This qualitative argument becomes more obvious when considering specific data points. Data points SWM03-01 and SWM02-04 are from filaments of different thickness, but show very similar values of concentration variance σ^2 , for example for potassium (Fig. 8, second panel). However, a single pulse origin would predict distinct values of σ^2 for filaments of different thickness. Especially for these very thin filaments the single-pulse regression curve ought to slope steeply, meaning a pronounced difference in σ^2 is expected (see Fig. 6). As the regressions in all major elements for the entire set of experimental filaments shows opposite curvature compared to the single-pulse case, more than one multi-pulse filament must be present in this set. The visual observations from 3D microCT analysis confirm this notion of multiple thin filaments converging to larger ones and therefore support the validity of correlating filament thickness with concentration variance to distinguish single and multi-pulse filaments. We therefore conclude that the proposed statistical treatment of compositional data of magmatic filaments is useful to constrain their formation mechanism. This is important as the exact mechanisms, time evolution and conditions of formation are essentially unknown for any natural sample. Therefore, magmatic filaments and their observed compositional patterns need to be tested for whether bubbles have played a role for magma mixing.

Referee #1: Table 1: These compositions are normalized. How were they measured? I realize that you are citing another paper but it is easy enough to indicate how they were measured (EMP I guess). [Authors' comments:] Accepted, the caption now reads: Composition of end-member glasses from the Snake River Plain measured by X-ray Fluorescence (data from Morgavi et al., 2013).

C827

Referee #1: Figures - see my uploaded PDF file of scanned figs with comments Please also note the supplement to this comment: <http://www.solid-earth-discuss.net/7/C627/2015/sed-7-C627-2015-supplement.pdf> Interactive comment on Solid Earth Discuss., 7, 1469, 2015. Comments addressing the reviewer's supplement on the figures:

[Authors' comments on figures:]

â€¢ Figure 1: We now added better indications to where interstitial air was trapped in the experimental charge. Furthermore, we added an arrow detailing the filament formation, as requested by the reviewer.

â€¢ Figure 2: A sketch has been added to Fig. 2 along with the following change to the corresponding figure caption: a) Sketch of filament formation by bubble ascent in side view and cross-section. Mafic melt is attached to bubble and dragged upwards by the buoyancy of the bubble. The column-like filament appears circular shaped in cross-section. b) Modelled compositional profile after the thin-source problem (e.g., Zhang 2010). Filament thickness is determined by selecting the inflection points of each profile. Gradient length denotes the part of the compositional profile, in which the composition shows variations.

â€¢ Figure 4: We agree with the reviewer that it would be better to include a sketch in this figure. However, we fear that this would make the rest of Figure 4 illegibly small. Instead we offer a new Figure 3, in which the 3D view and the horizontal sections are better tied together. Also, the caption of Figure 4 has been rewritten, and we have additionally included a reference to Figure 3: Backscattered electron images of horizontal sections of experimental glass. a) uppermost, b) intermediate and c) lowermost section of the rhyolite glass (dark grey), which contains horizontally sectioned magmatic filaments in light grey. Yellow lines indicate the locations of the EMP transects. Please refer to Figure 3 for the exact vertical location of each section. The BSE images are complemented by representative major element concentration profiles. Blue and red lines indicate the initial compositions of the end-members basalt and rhyolite. In response to the reviewers comment, we also improved Figure 3 by adding the BSE images of the filament structures. Additionally, the caption to Fig. 3 has been improved: Figure 3: a)

C828

3D representation of the experimental charge. The lower yellow layer is basaltic glass, whereas the upper rhyolitic layer has been rendered transparent. Hybrid material was rendered orange as a result of differing attenuation behaviour. The experimental charge has subsequently been sectioned parallel to the basalt-rhyolite interface at three levels, indicated by the red ellipses. The resulting cross-sections of the filament structures are shown as back-scattered electron images obtained from EMP analysis: b) SWM-01, c) SWM-02, and d) SWM-03.

â€¢ Figure 5: Well spotted! A very good comment. This non-linearity is due to diffusive fractionation of species and has been discussed in previous publications from our group (e.g. Perugini et al., 2006; De Campos et al., 2008; Perugini et al., 2008). Relative changes in diffusivity of Na and K, both of which contribute to the y-axis in a TAS plot, cause a deviation from linear mixing behaviour on short length-scales. As this effect has been discussed at length in previous publications, we offer to include the following sentence in the caption of Fig. 5 to refer back to these studies: TAS plot of end-member compositions and hybrid compositions produced during the bubble advection experiment. Data normalised to 100% totals. Blue and red circles denote the end-member compositions of Snake River Basalt and Rhyolite. Non-linearity of trend is due to diffusive fractionation of Na versus K (see Perugini et al., 2006; De Campos et al., 2008; Perugini et al., 2008).

â€¢ Figure 6: Y-axis label corrected and captions reversed between Figs. 6 and 7.

â€¢ Figure 7: Captions reversed between Figs. 6 and 7.

â€¢ Figure 9: Judging from the scanned print-out, which the reviewer commented on, we believe the figure was initially of too low contrast. We now increased the contrast of Fig.9 and reduced it, so the filament becomes very obvious. We also stress that this glass sample from Axial seamount has actually been measured for its composition and the filament is clearly of more mafic composition than the surrounding melt. We also clarified the main text with respect to this.

Please also note the supplement to this comment:
<http://www.solid-earth-discuss.net/7/C820/2015/sed-7-C820-2015-supplement.pdf>

C829

C830

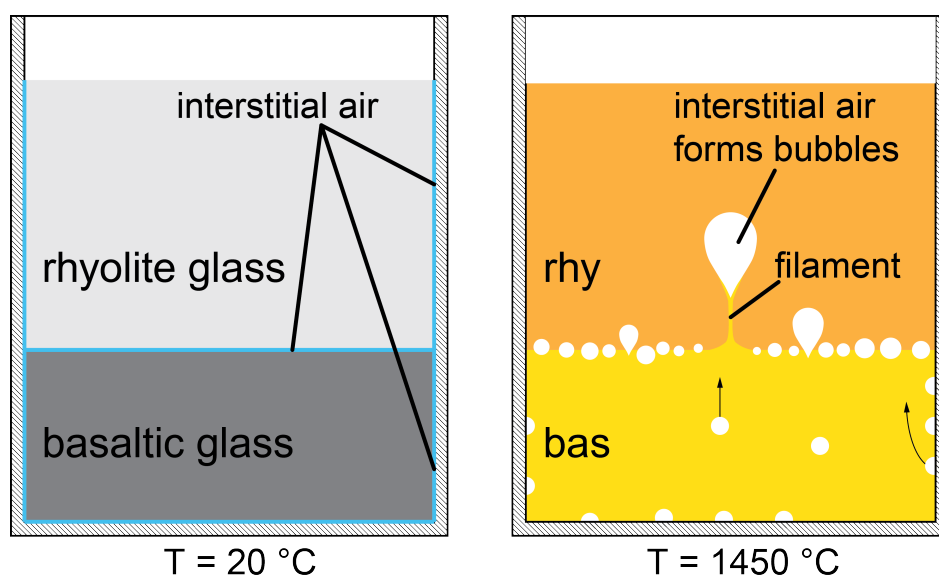


Fig. 1. Experimental set-up

C831

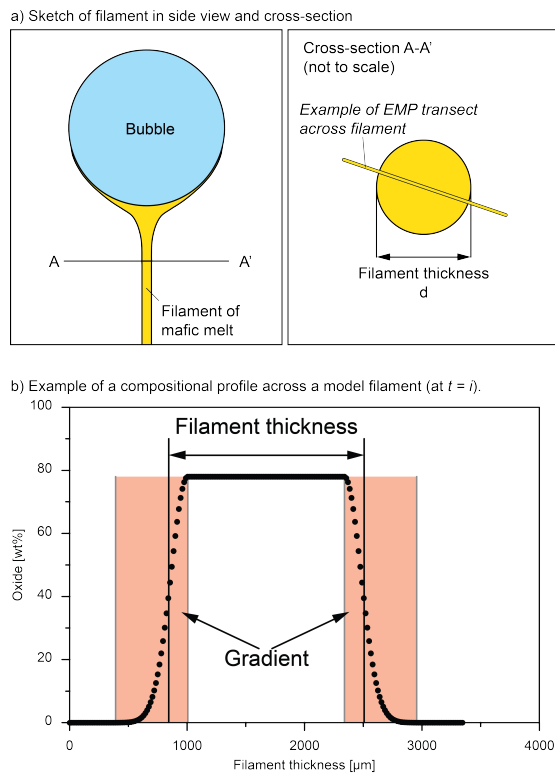


Fig. 2. Model filament

C832

3D view of run product:

BSE images of cross-sections:

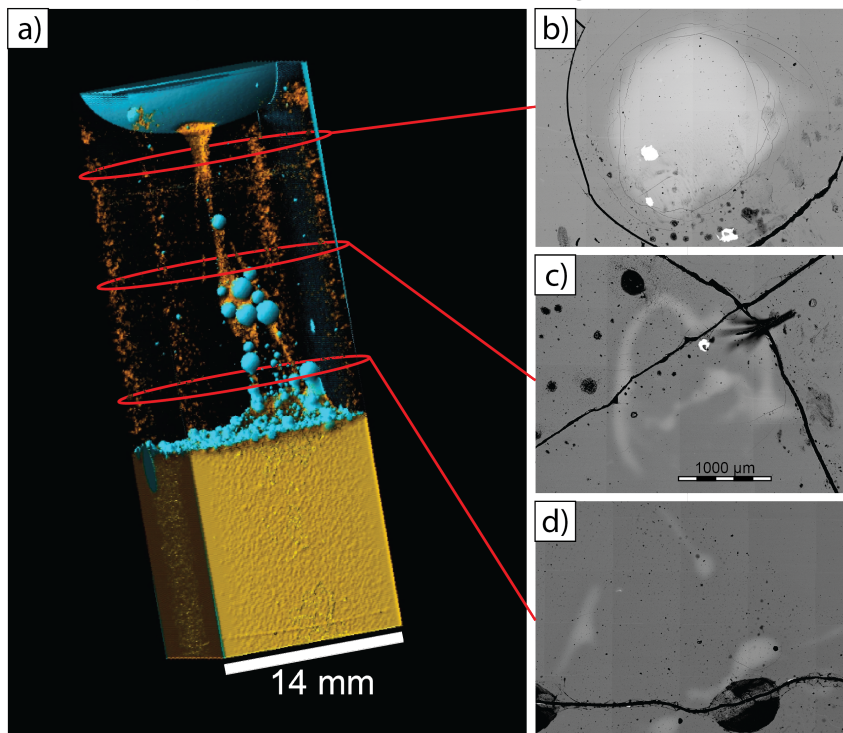


Fig. 3. 3D view and sections

C833

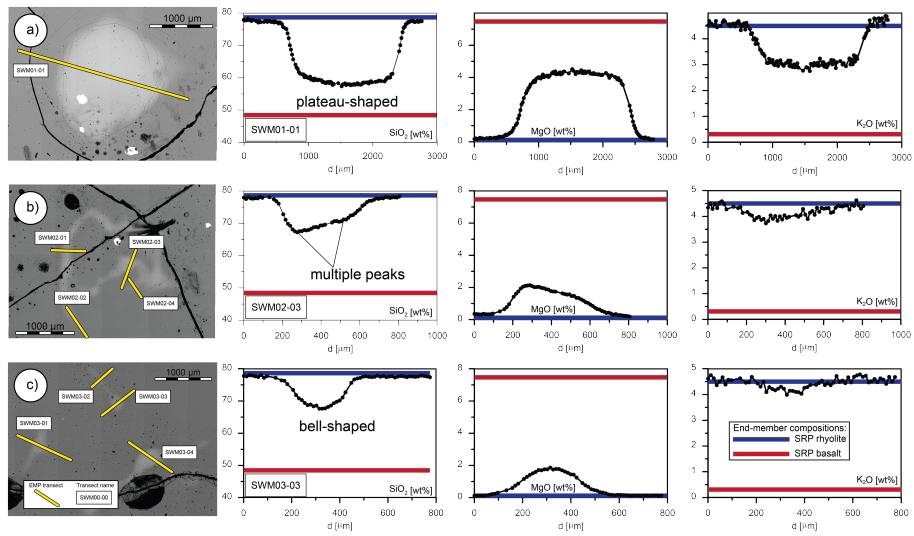


Fig. 4. BSE images and EMP profiles

C834

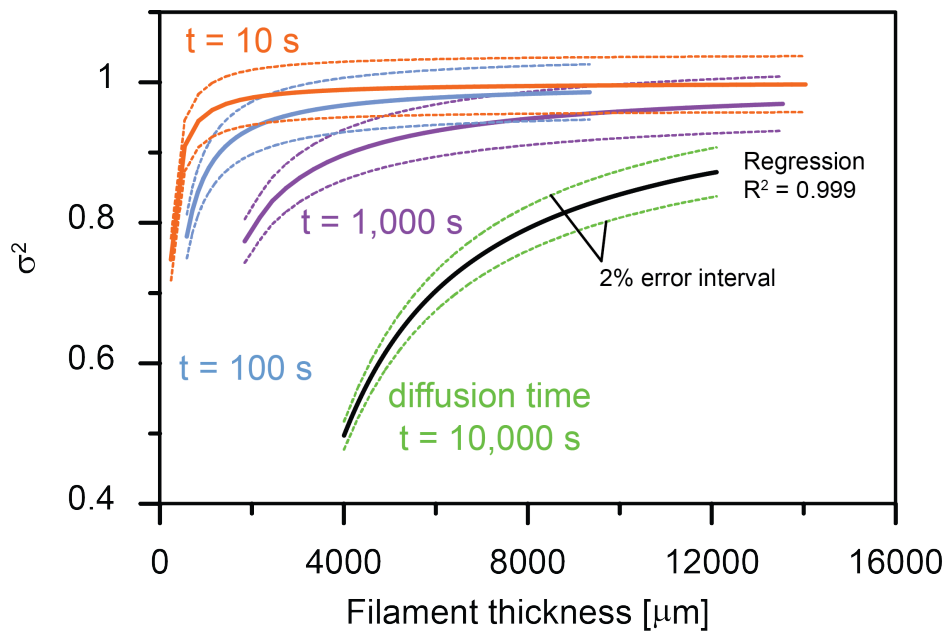


Fig. 5. new Figure 6: Model filament thickness vs. concentration variance

C835

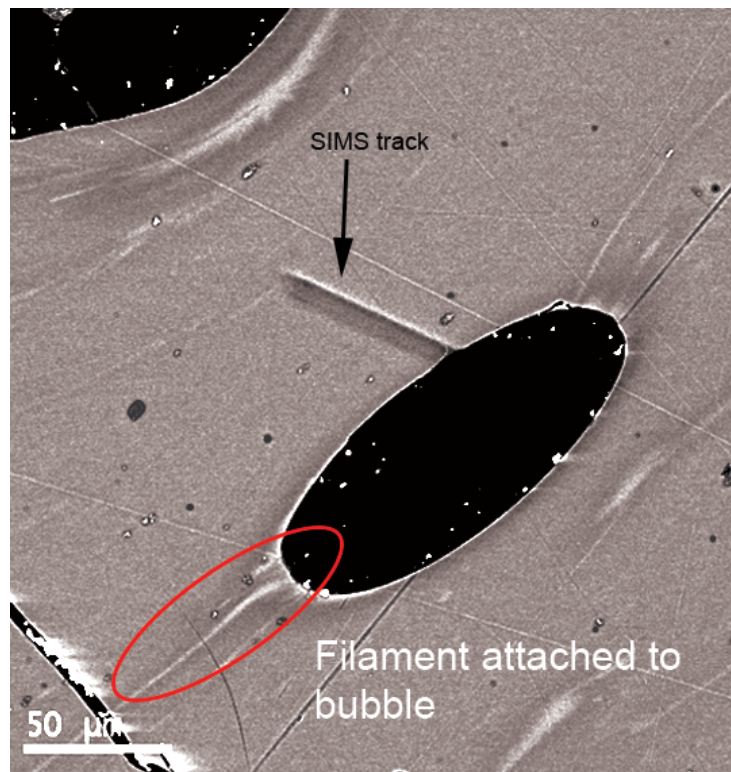


Fig. 6. new Figure 9: BSE image of Axial seamount glass

C836